



# Magnetic and structural studies of nickel-substituted cobalt ferrite nanoparticles, synthesized by the sol–gel method

M. Mozaffari\*, J. Amighian, E. Darsheshdar

Department of Physics, Faculty of Science, University of Isfahan, 81746-73441, Isfahan, Iran

## ARTICLE INFO

### Article history:

Received 14 May 2012

Received in revised form

26 June 2013

Available online 3 September 2013

### Keywords:

Sol–gel method

Nanoparticle

Nickel substituted cobalt ferrite

Magnetic property

Superexchange interaction

Magnetic anisotropy energy

## ABSTRACT

In this study Ni substituted cobalt ferrite nanoparticles ( $\text{Ni}_x\text{Co}_{1-x}\text{Fe}_2\text{O}_4$  where  $x=0.1, 0.3, 0.5, 0.7$  and  $0.9$ ) were prepared by the sol–gel method. Phase identification of the samples was performed by the X-ray diffraction (XRD) method and the mean crystallite sizes of the samples were obtained using Scherrer's formula. The results show that a minimum calcining temperature of  $500^\circ\text{C}$  is required to obtain single phase spinel structures for all the samples. It was observed that the lattice parameter of the samples decreases from  $8.350$  to  $8.300\text{ \AA}$  with increasing Ni content. Morphology of the samples was investigated by a field emission scanning electron microscope (FESEM). Also mean particle sizes of the samples were obtained from FESEM images and there no relation between particle size and Ni content was found. Magnetic measurements were carried out on the cold pressed samples and the results show that saturation magnetization decreases as  $x$  increases. Curie temperatures of the samples were determined and the results show that by increasing  $x$  values their Curie temperatures increase. This increase was explained based on the change in superexchange interactions between magnetic ions by substitution of Ni ions in Co ferrite. Also the coercive forces of the samples decreased with increasing  $x$  values which was explained by the changes in magnetocrystalline anisotropy.

© 2013 Elsevier B.V. All rights reserved.

## 1. Introduction

Ferrite nanoparticles are of great interest because of their scientific aspects and applications in permanent magnets, targeted drug delivery, and high-density information storage devices. From crystal structure point of view, ferrites are generally divided into two groups: cubic or spinel ferrites and hexagonal or hexaferrites [1,2].

Cobalt ferrite is a well-known hard magnetic material with a high coercivity and a moderate magnetization. These properties, along with its great physical and chemical stabilities, make  $\text{CoFe}_2\text{O}_4$  nanoparticles suitable for many practical applications such as audio/video tapes, high density digital recording disks, etc. [3–5]. On the other hand nickel ferrite is a typical soft magnetic material [6], which has many applications in electronic devices, such as inductors and transformer cores.

Nickel-substituted cobalt ferrites are highly resistive and magnetostrictive. Studies of Van Uitert and Jiang showed that a very large increase in the room-temperature resistivity of nickel ferrite is achieved by substituting one or two percent of cobalt ions [7–10].

In this investigation Ni substituted cobalt ferrite nanoparticles were prepared by the sol–gel method and their structure and morphology were studied by X-ray diffraction and FESEM respectively. Magnetic

properties of the samples were investigated from hysteresis loops and  $M$ – $T$  curves.

## 2. Experimental

To synthesize nickel-substituted cobalt ferrite nanoparticles stoichiometric amounts of nickel, cobalt and iron nitrates and citric acid, all from Merck Co. with minimum purity of 99%, were dissolved in distilled water and stirred to obtain homogenous clear sols. The obtained sols were heated at  $80^\circ\text{C}$  for 3 h on a hot plate magneto-stirrer and continuously stirred to obtain uniform gels. The obtained gels were then heated at  $100^\circ\text{C}$  for 48 h. The dried gels were milled for 0.5 h in a mortar. The prepared powders were calcined at  $200$ – $500^\circ\text{C}$  for 3 h. XRD patterns of the samples were obtained by a diffractometer (Bruker ADVANCED D8) with  $\text{Cu K}\alpha$  ( $\lambda=1.5406\text{ \AA}$ ) radiation. Mean crystallite sizes of the samples were estimated from broadening of the most intense XRD peaks, using Scherrer's formula

$$D = 0.9\lambda / (B \cos \theta_B) \quad (1)$$

where  $\lambda$  is X-ray wavelength,  $B$  is line broadening (just due to crystallite size) and  $\theta_B$  is the Bragg angle. Total broadenings ( $B$ ) of the XRD peaks are due to crystallite size, instrument and strains.

\* Corresponding author. Tel./fax: +98 311 793 4741.

E-mail addresses: [mozafari@sci.ui.ac.ir](mailto:mozafari@sci.ui.ac.ir), [mmozafari@hotmail.com](mailto:mmozafari@hotmail.com) (M. Mozaffari).

For annealed powders the latter one can be ignored. But to consider the instrumental broadening we applied Warren's correction formula

$$B'^2 = B_m^2 - B_s^2 \quad (2)$$

where  $B_m$  is broadening of a peak in the XRD pattern and  $B_s$  is broadening of the same peak obtained from XRD pattern of a standard bulk powder with crystallite size greater than 1  $\mu\text{m}$ . To apply Warren's correction,  $B$  in Eq. (1) should be replaced by  $B'$  in Eq. (2) [11]. Morphology of the samples was investigated by a field emission scanning electron microscope (FESEM). Hysteresis loops of the samples were recorded on the cold pressed powders at room temperature in an applied magnetic field with a maximum of 12 kOe, using a sensitive permeameter. Curie temperatures of the samples were also determined, using a sensitive Faraday balance, by placing the samples in a nonhomogeneous magnetic field and measuring the force which the samples experience.

### 3. Results and discussion

XRD patterns of the dried gels before calcinations did not show any peaks because at this stage the required thermal energy was not sufficient. XRD investigations of the samples calcined at different temperatures from 200 to 400  $^{\circ}\text{C}$  show that in addition to desired spinel phase a minor undesired hematite phase has been formed. Fig. 1 shows a typical XRD pattern related to the sample with  $x=0.5$  calcined at 200  $^{\circ}\text{C}$ . Fig. 2 shows XRD patterns of the samples calcined at 500  $^{\circ}\text{C}$ . As can be seen by increasing the calcining temperature to 500  $^{\circ}\text{C}$ , all the samples become single phase and the minor undesired hematite phase disappears. So all the measurements were carried out on these samples and the subsequent results are related to them. Calculated lattice parameters are tabulated in Table 1. As can be seen lattice parameter decreases with increasing nickel content, which can be explained based on substitution of  $\text{Ni}^{2+}$  with a smaller ionic radius (0.69  $\text{\AA}$ ) for  $\text{Co}^{2+}$  with a larger ionic radius (0.74  $\text{\AA}$ ) [1].

Mean crystallite sizes of the samples were calculated by Scherrer's formula, using Warren's correction and they are about 30 nm for all samples. FESEM images of the samples are shown in Fig. 3. As can be seen all the samples have nearly homogeneous particles. Particle sizes of the samples were calculated from FESEM micrographs, by numbering of at least 100 particles, and they are tabulated in Table 1. As can be seen the mean particle sizes were in

the range of 70–160 nm. As the mean crystallite sizes of the samples were about 30 nm, it shows that each particle contains several crystallites.

Fig. 4 shows room temperature  $M-H$  loops of the samples ( $\text{Ni}_x\text{Co}_{1-x}\text{Fe}_2\text{O}_4$ ) with different  $x$  values. As can be seen coercivities of the samples decreased with increasing  $x$  values. This is due to lower magneto-crystalline anisotropy of  $\text{Ni}^{2+}$  with respect to that of  $\text{Co}^{2+}$  [12]. Table 2 also shows the decrease of  $M_s$  values of the samples as the nickel content ( $x$ ) increases. A similar trend of decrease in saturation magnetization with Ni substitution in Co ferrite has been reported by others who prepared their samples with different routes, forced hydrolysis [13] and mechanochemical [14]. This decrease in  $M_s$  with increasing Ni content is attributed to the smaller magnetic moment of  $\text{Ni}^{2+}$  ( $2 \mu_B$ ) as compared to larger magnetic moment of  $\text{Co}^{2+}$  ( $3 \mu_B$ ). If one assumes  $\text{Fe}^{3+}$  ( $5 \mu_B$ )

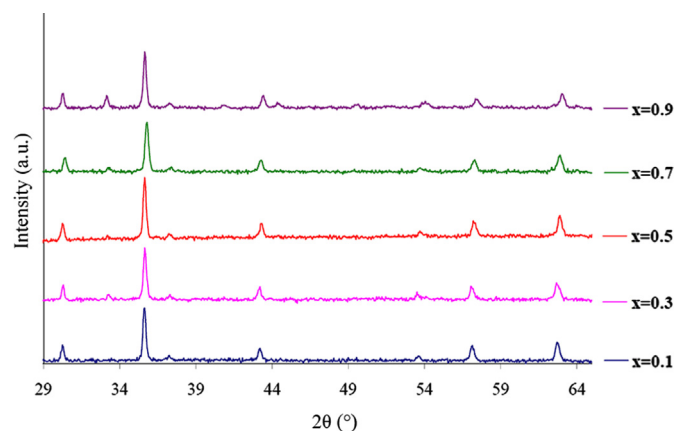


Fig. 2. XRD patterns for the samples calcined at 500  $^{\circ}\text{C}$ .

Table 1

Lattice parameter and particle size of the samples.

Sample	$a$ ( $\pm 0.001$ $\text{\AA}$ )	Particle size ( $\pm 2$ nm)
$\text{Ni}_{0.1}\text{Co}_{0.9}\text{Fe}_2\text{O}_4$	8.350	120
$\text{Ni}_{0.3}\text{Co}_{0.7}\text{Fe}_2\text{O}_4$	8.340	160
$\text{Ni}_{0.5}\text{Co}_{0.5}\text{Fe}_2\text{O}_4$	8.335	150
$\text{Ni}_{0.7}\text{Co}_{0.3}\text{Fe}_2\text{O}_4$	8.312	80
$\text{Ni}_{0.9}\text{Co}_{0.1}\text{Fe}_2\text{O}_4$	8.300	70

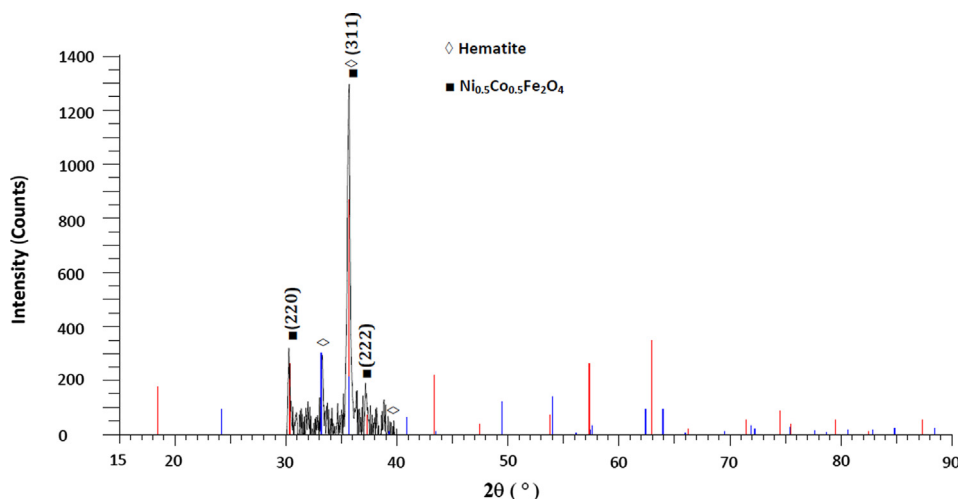


Fig. 1. Typical XRD pattern for one of the samples ( $x=0.5$ ), calcined at 200  $^{\circ}\text{C}$ .

Download English Version:

<https://daneshyari.com/en/article/8157564>

Download Persian Version:

<https://daneshyari.com/article/8157564>

[Daneshyari.com](https://daneshyari.com)